Research Article | Vol. 31, No. 23 / 6 Nov 2023 / Optics Express 38786
Optics EXPRESS

Monolithic VECSEL for stable kHz linewidth

MARTIN LEE, PAULO HISAO MORIYA,* AND JENNIFER E. HASTIE

Institute of Photonics, Department of Physics, SUPA, University of Strathclyde, Technology and Innovation Centre, 99 George Street, Glasgow G1 1RD, UK
*paulo.moriya@strath.ac.uk

Abstract: Vertical-external-cavity surface-emitting semiconductor lasers (VECSELs) are of increasing interest for applications requiring ultra-coherence and/or low noise at novel wavelengths; performance that is currently achieved via high-Q, air-spaced resonators to achieve long intra-cavity photon lifetimes (for the so-called class-A low noise regime), power scaling and high beam quality. Here, we report on the development of a compact, electronically tunable, *monolithic-cavity*, class-A VECSEL (monolithic VECSEL) for ultra-narrow free-running linewidths. A multi-quantum-well, resonant periodic gain structure with integrated distributed Bragg reflector (DBR) was optically-bonded to an air-gap-free laser resonator created inside a right-angle fused-silica prism to suppress the influence of environmental noise on the external laser oscillation, thus achieving high stability. Mode-hop-free wavelength tuning is performed via the stabilized temperature; or electronically, and with low latency, via a shear piezo-electric transducer mounted on the top of the prism. The free-running linewidth, estimated via the frequency power spectral density (PSD), is sub-kHz over ms timescales and <1.9 kHz for time sampling as long as 1s, demonstrating at least two orders-of-magnitude improvement in noise performance compared to previously reported single frequency VECSELs. The stable, total internal reflection resonator concept is akin to the prevalent monolithic non-planar ring oscillator (NPRO), however the monolithic VECSEL has several important advantages: tailored emission wavelength (via semiconductor bandgap engineering), no relaxation oscillations, no applied magnetic field, and low requirements on the pump beam quality. This approach is power-scalable in principle and could be applied to VECSELs at any of the wavelengths from the visible to the mid-infrared at which they are already available, to create a range of robust, ultra-coherent laser systems with reduced bulkiness and complexity. This is of particular interest for remote metrology and the translation of quantum technologies, such as optical clocks, from research laboratories into real world applications.

1. Introduction

Ultra-stable and coherent lasers are the cornerstone of several modern technologies with applications in precision spectroscopy [1], LiDAR [2], interferometry [3], quantum communications [4], and quantum technologies (QT), such as optical clocks [5] used for metrology [6]. For example, blue and red lasers with linewidths from MHz down to sub-Hz are used in neutral strontium optical lattice clocks, which are predicted to have superior accuracy and lower instability than current microwave standards, and are a leading candidate for redefining the SI 'second' [7,8]. The transition of QT systems from laboratory-based setups to portable and deployable devices is directly dependent on the development of portable, highly-coherent light sources with reduced size, weight, power, and costs (SWaP-C) without loss of performance, as lasers are responsible for a significant portion of the overall QT apparatus footprint.

#490046 https://doi.org/10.1364/OE.490046
Journal © 2023 Received 22 Mar 2023; accepted 24 Oct 2023; published 1 Nov 2023

Optics EXPRESS

Solid-state [9] and fiber [10] lasers can provide high power and stability but can suffer from large SWaP-C and limited wavelength coverage. As a result, semiconductor laser systems, such as extended cavity diode lasers (ECDLs), are widely used due to broad spectral coverage, especially in the near and mid infra-red (IR), but suffer from poor beam quality, and intrinsically high frequency, phase, and intensity noise. External amplification, non-linear conversion modules, and frequency stabilization stages [11] are often required for power scaling, wavelength coverage expansion, and linewidth narrowing, respectively, but also increase the laser system footprint. More recently, on-chip hybrid integration of semiconductor lasers with ultra-high-Q waveguide resonators is being used to develop highly compact, ultra-narrow linewidth light sources [12]. Silicon nitride waveguides offer broad transparency and the resonators suppress the intrinsically high frequency noise of the laser diode (~MHz) [13]. On the other hand, optically-pumped vertical-external-cavity surface-emitting lasers (VECSELs) [14], which have a spontaneous emission factor many orders of magnitude lower than in-plane semiconductor lasers, have intrinsically *low* frequency noise and can achieve high power (multi-Watt) single frequency operation while maintaining high brightness (TEM_{00}, $M^2 \leq 1.1$), see e.g. [15]. Further, for VECSEL cavity lengths of 10s of mm or more, the external cavity photon lifetime exceeds the gain lifetime (few ns) ensuring low intensity noise without relaxation oscillations, resulting in so-called class-A laser dynamics [16]. The fundamental (or Schawlow-Townes-Henry) linewidth limit [17,18] for VECSELs is predicted to be sub-Hz, typically broadened by environmental noise acting on the air-spaced laser resonator and injection of pump intensity noise; however, with the high finesse external laser cavity acting as a low-pass filter, the pump-related noise transfer is limited to those frequencies below the cavity cut-off frequency. Measurements of the broadened laser linewidth are therefore dependent on the integration time, with confirmation of stable sub-kHz linewidth requiring measurements of at least 1 s to avoid under sampling the noise at low frequencies [19]. Optimization of the VECSEL architecture has resulted in reported free-running (i.e. without active frequency stabilization) linewidth of 21 kHz for a sampling time of 1 ms, increasing to 995 kHz at 1 s for an InGaAs-based VECSEL emitting at wavelengths around 1 μm [20], and in our previous work, < 150 kHz for 2s with a low noise pump laser [21]. When frequency-stabilized to counteract pump, thermal, and mechanical noise, we have recently demonstrated sub-200 Hz linewidth operation over sampling times of up to 1000 s with a GaInP/AlGaInP-based VECSEL at 689 nm [21], suitable for cooling neutral strontium atoms.

Narrower free-running linewidths can be demonstrated when the influence of external noise (e.g., thermal and mechanical) in the laser resonator is reduced. An interesting method is the use of monolithic-cavity architecture, which offers a robust approach to reducing the impact of environmental noise on the laser field whilst also providing a compact and rugged package. This type of architecture has been successfully implemented in solid-state lasers delivering stable narrow-linewidth operation [22,23]. In particular, commercial non-planar-ring-oscillators (NPROs) can achieve high power and low free-running linewidths of a few kHz (typically 2-5 kHz) without the addition of complex stabilization techniques [24]. By containing the oscillating field within a polished monolithic gain crystal, NPROs significantly reduce resonator path length instabilities due to vibration and thermal drifts. The optical gain in a NPRO comes from the resonator substrate, typically Nd:YAG or Yb:YAG, limiting the spectral coverage available from these lasers. Unidirectional oscillation must be enforced to avoid spatial hole burning in the gain crystal; NPROs therefore require a non-reciprocal polarization rotation for the two propagation directions inside the resonator [25], which is achieved via magnetic fields, non-planar geometry, and polarization sensitive coatings. Furthermore, NPROs suffer from relaxation oscillations inherent to the long upper-state lifetime of the solid-state gain crystal, which must be removed by intensity stabilization (so called noise-eaters). Whilst monolithic cavities have previously been demonstrated with microchip VECSEL technology [26], the sub-mm cavity lengths did not

Optics EXPRESS

provide sufficient cavity photon lifetimes to oscillate under class-A carrier dynamics, making them unsuitable for low noise operation.

Here we present a novel approach to delivering a diode-pumped, monolithic-cavity laser for applications requiring high brightness and coherence at novel wavelengths. Using a high-tolerance right angle prism, a monolithic VECSEL cavity has been designed and built to take advantage of both the intrinsically narrow linewidth and class-A dynamics of this technology, achieving free-running linewidth <1.9 kHz for sampling times as long as 1 s. The hybrid laser architecture proposed here offers the unique ability to combine the stability benefits of a NPRO with the wavelength coverage of semiconductor lasers, relaxation-oscillation-free dynamics, and a reduced complexity of the monolithic-cavity design (no need for enforced unidirectional oscillation or magnetic fields). This results in a robust, wavelength flexible laser platform that is favorable for use in extreme environments, such as space-based applications, where NPROs are frequently successfully deployed [27,28].

2. VECSEL gain structure and laser cavity considerations

2.1. VECSEL gain structure and monolithic cavity architecture

The VECSEL gain mirror used here is similar to those previously reported by our group [21], designed for absorption of green pump light in the quantum well barrier layers (at around 532 nm) and laser emission at around 674 nm. The gain region is formed by 20 compressively-strained GaInP quantum wells, grouped in pairs and separated by AlGaInP barrier layers for resonant periodic gain (RPG), grown on top of a high reflectivity (calculated to be > 99.98%) distributed Bragg reflector (DBR) mirror composed of 32.5 periods of AlGaAs/AlAs layers. A 4×4 mm^2 sample was selected, then the epitaxial surface was capillary-bonded to an optical grade single crystal synthetic diamond heat spreader (0.5–mm-thick, 4-mm-diameter) for thermal management (see Fig. 1(c)).

In its simplest form, a linear monolithic-cavity VECSEL (monolithic VECSEL) can be constructed by placing a low loss optical substrate of sufficient length between the VECSEL gain mirror and output coupling mirror. However, clear access for the propagation of the optical pump beam through the monolithic cavity (see Fig. 1(a)) is required for those gain structures where the substrate and DBR are not transparent at the pump wavelength and must therefore be pumped via the emission surface, adding an additional requirement to the monolithic geometry. Making use of commercially available optical components, with the ability to optically-bond these components into more complex folded resonators, prototype monolithic designs can be produced in a much more cost-effective manner than bespoke single optics. Such an approach was previously demonstrated, for example, for a mode-locked Yb:Er:glass laser where a variety of CaF_2 optics were bonded together to form the low noise, monolithic laser cavity [29]. Most commercial optical components will have sufficiently high surface quality to permit strong optical contact bonding, minimizing any interface losses to the laser field. Additionally, the epitaxially-grown VECSEL gain mirrors are atomically flat making them suitable for capillary- or chemically-activated bonding - indeed, VECSELs routinely have transparent crystalline heat-spreaders bonded to the top or bottom surface of the gain mirror, as here, to provide efficient heat removal [21,30].

The VECSEL cavity (see Fig. 1(a)) was formed between the gain mirror DBR (see Fig. 1(c)) and a fused silica, plano-convex output coupler (ø = 12.7 mm, RoC = 40 mm and thickness = 3 mm), coated on the convex surface for 1% transmission at wavelengths between 650-700 nm. A high precision, uncoated UV-fused silica right-angle prism was selected as the laser cavity spacer to ensure near perfect cavity alignment and lossless optical bond interfaces. With this scheme, the intra-cavity field undergoes four total internal reflections (TIR) per round trip. Furthermore, the prism geometry gives easy access for the pump laser to be aligned to the VECSEL gain mirror through one of the exposed arms of the prism. This relatively standard, off-the-shelf

Optics EXPRESS

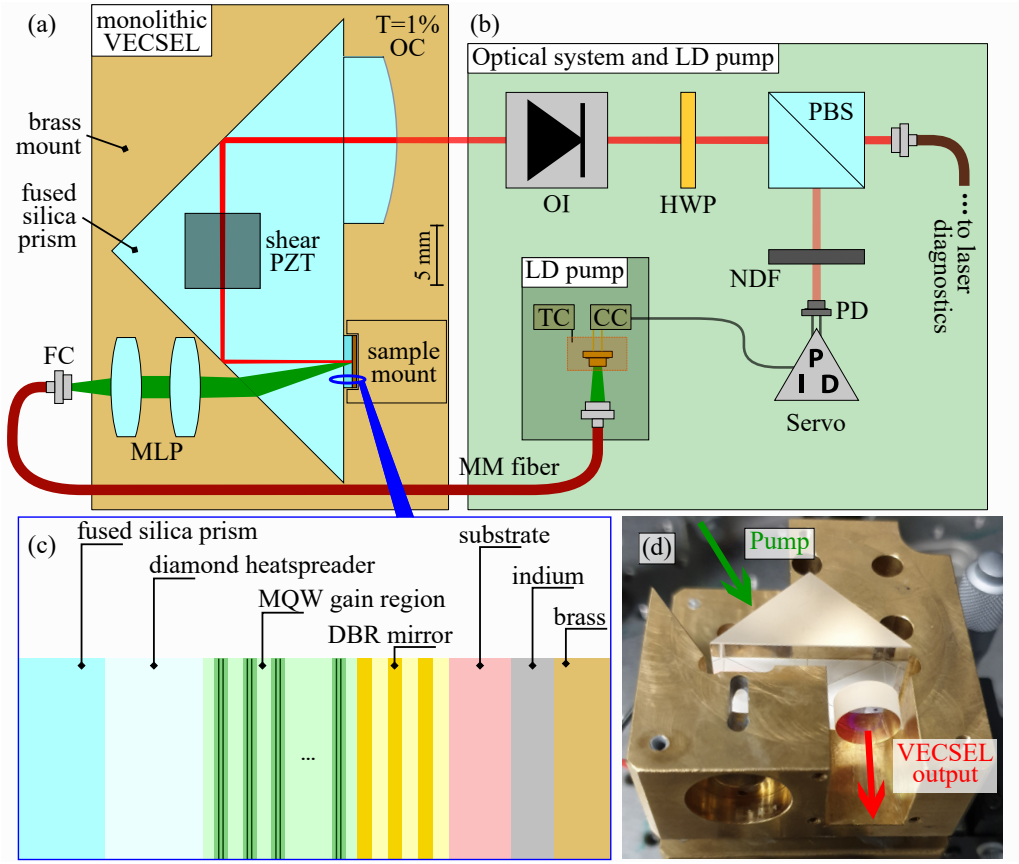

Fig. 1. (a) Top view illustration (to scale) of the right-angle-prism-based monolithic VECSEL. Each of the four optical components – the VECSEL gain mirror, a diamond heat spreader, the 25 mm right-angle prism, and a planar-convex output coupling mirror – are shown bonded together to form the complete optical cavity, mounted on a brass housing. The optical paths within the structure for both the green pump beam and the red oscillating laser field are shown in the image (both not to scale). (b) Schematic (not to scale) of the measurement system (green box) and the pump laser (dark green box). The VECSEL output is split and distributed to: diagnostic equipment for characterization of output power, emission spectrum, intensity and frequency noise; and a photodetector (PD) for correction of the pump intensity noise. The pump is based on a green laser diode, with the pump beam delivered to the gain structure via a 50 µm multimode fiber. (c) Schematic of the VECSEL semiconductor gain structure. (d) Brass mounting block is shown with the monolithic cavity in-situ before bonding of the shear PZT and lid. The output coupler can be seen bonded onto the hypotenuse of the prism. FC: fiber coupler; MLP: matched lens pair; PZT: piezo electric transducer; OC: output coupler; OI: optical isolator; HWP: half-wave plate; PBS: polarizing beam splitter; NDF: neutral density filter; PD: photodiode; MM fiber: multimode fiber; LD: laser diode; CC: current controller; TC: temperature controller; DBR: distributed Bragg reflector; MQW: multi-quantum well.

Optics EXPRESS

component has an arm length of $L_p = 25$ mm and angular tolerance of 15 arcseconds and λ/20 surface flatness. Fused silica also has a low thermal expansion coefficient (0.55×10^{-6} °C^{-1}), helping to reduce any thermal lensing effects that may arise during optical pumping, and a large transparency window with low absorption loss, especially at visible wavelengths. All surfaces of the prism remained uncoated, leading to Fresnel reflection loss at the air-prism interface for the pump beam (R ≈ 4%); however, this could be readily minimized in future work with a standard AR coating. Both output coupler and heatspreader were optically contact bonded onto the hypotenuse of the prism, ensuring overlap with the optical axis of the output coupler, thus setting the resonator mode and cavity length without the possibility of further adjustments. The optical path of the pump laser (green) and oscillating field (red) is shown in Fig. 1(a).

The resonator design and substrate material were selected to ensure class-A dynamics, i.e. intra-cavity photon lifetime (τ_p) greater than the active medium carrier lifetime (τ_e). The carrier lifetime is assumed to be on the order of a few ns, as is typical with III-V semiconductor quantum wells [14]. For the monolithic VECSEL presented here, the total cavity length is L = 38.85 mm, including the path length inside the prism ($\sqrt{2} \times L_p \approx 35.35$ mm), the crystalline heatspreader (0.5 mm) and T = 1% output coupler thickness (3 mm), thus ensuring class-A dynamics with a photon lifetime > 30 ns (ignoring interface losses).The monolithic cavity was placed in a temperature-stabilized brass housing (see Fig. 1(d)) with mK precision via thermo-electric cooling (temperature controller: Thorlabs Inc., TED4015), with thermal contact between the gain mirror substrate and the brass improved with a layer of indium foil (Fig. 1(c)). The heat generated by the optical pumping process, focused in a 50 μm spot near the epitaxial surface of the semiconductor gain mirror (see Section 3.1), is dissipated by the diamond heatspreader into the fused silica prism but also transferred to the brass mount through the gain mirror substrate [29]. A detailed analysis of the thermal transport mechanism in VECSEL structures with intracavity heatspreaders can be found in [31]. The thermal performance of the monolithic-cavity could perhaps be improved in future designs via direct contact between the diamond and the brass mount. Finally, a shear piezo-electric transducer (Thorlabs PL5FBP3, 5×5 mm^2, thickness = 1.8 mm; shown in Fig. 1(b)) was bonded to the top of the prism and to the lid of the housing for electronic tuning purposes.

2.2. Polarization considerations

The optical field inside the monolithic cavity has an incident angle of 45° at the total internal reflections, which ensures a non-zero phase rotation between the s and p polarizations. In a laser cavity, the polarization must repeat after every round trip and the phase must equal an integer value of 2π [25,32]. For this resonator, this condition is only fulfilled for the pure p or s states, or [1,0] and [0,1], respectively, with all other linear polarization states becoming elliptical from the phase rotation and therefore strongly suppressed. Since the cavity provides no additional loss for either allowed polarization state, the final selection of the laser polarization is set by a combination of any residual birefringence in the diamond heat spreader [33] and anisotropy in the quantum well gain [34]. The former is related to residual strain from defects during CVD growth of single crystal diamond resulting in a small birefringence in the diamond (n_e - $n_o < 10^{-5}$). The latter is attributed to symmetry breaking between the [110] and [1$\bar{1}$0] axes and strain fields in the material from the small lattice mismatch between the barrier and the quantum well layers. Theoretical calculations for III-V ternary material and experimental results for InGaAs-based VECSEL gain mirrors have shown an approximate 10% difference in gain between the polarization directions [34], which is more than sufficient discrimination to fix the polarization of the low gain laser.

Optics EXPRESS

3. Monolithic VECSEL operation and characterization

3.1. Pump laser systems

Two pump laser systems were used: a commercial optically-pumped semiconductor laser, or OPSL, (Coherent Inc., Verdi G5) with output power of up to 2.5 W at 532 nm, and a multimode, multi-emitter green laser diode (Nichia Corp., NDG7D75) emitting up to 1.2 W at 520 nm [35]. The former pump laser was free-space-aligned and focused into the gain structure using a single lens, was used solely to investigate only the power scaling of the fixed resonator. The latter, used to reduce the overall laser system SWaP-C, was first coupled into a multimode fiber (core size = 50 µm) before being sent to the gain structure through a lens pair ($f_1 = f_2 = 25$ mm), re-imaging the fiber core to a spot size measured to be approximately 51 µm. After the fibre-coupling was implemented, a maximum of 0.86 W of green laser power was available for optical pumping. Pump intensity-stabilization can be implemented via a correction signal applied to the pump diode current (see Fig. 1(a)-(b)), helping to reduce the injection of intensity noise into the VECSEL [35]. This can be monitored by sampling the pump intensity noise directly from the Fresnel reflection off the diamond heatspreader, as in Ref. [35]; however, here it was more convenient to sample the VECSEL output. The pump intensity noise is directly transferred to the VECSEL up to the cut-off frequency of the laser cavity (4.3 MHz in this case) [16]. In both cases, the angle of incidence of the pump laser beam in the prism and the gain structure are around 30° and 14°, respectively.

3.2. Laser performance characterization

Careful alignment is required to achieve good mode-matching of the pump focus to the intracavity mode size at the gain mirror, which in this case is set by the fixed resonator to be 53 µm. First, the OPSL beam was focused down to approximately 68 µm on the gain mirror when using a 180 mm lens. The power transfer for this configuration is shown in Fig. 2(a), showing multimode output of 78 mW with a threshold of (0.57 ± 0.01) W and a conversion efficiency of (7.4 ± 0.1) %. Power scaling while maintaining single mode operation would require an adjustment to the monolithic geometry to achieve a larger mode size at the gain mirror.

The power performance of the monolithic VECSEL when pumped with the laser diode is also shown in Fig. 2(a), in this case for single-frequency operation, confirmed via the transmission of a scanning Fabry-Perot cavity (see Section 4). A peak output power of 19 mW was measured with a slope efficiency of (9.1 ± 0.1) % and threshold of (0.67 ± 0.06) W, with no thermal rollover observed. It is important to highlight here that single frequency operation was achieved while diode pumping due to the elimination of higher order transverse modes in the VECSEL cavity by improving the cavity mode and pump spot size overlap ratio from 0.78 to 0.96 when OPSL and diode pumping, respectively [36]. In addition, the increased slope efficiency over that measured with the OPSL pump can be attributed to better matching of the pump focus to the fixed cavity mode size, provided by the smaller pump spot size. The monolithic VECSEL operated at 672 nm with a circularly symmetric TEM_{00} output beam (see Fig. 2(b)).

In contrast to air-spaced configurations, no intracavity filtering is implemented for wavelength tuning. In the monolithic VECSEL the emission wavelength can be tailored via band gap engineering in the design of the gain mirror, gain mirror temperature, and thermal control of the cavity substrate (in our case fused silica), with a wavelength tunability of (2740 ± 30) MHz/°C measured (see Fig. 2(c)). For the remaining characterization, the monolithic VECSEL mount temperature was kept at 16 °C. Additionally, finer wavelength tuning was performed via the shear PZT bonded to the top surface of the right-angle prism. In this case a maximum tunability of 40.5 MHz was measured when a 1 Hz triangle wave signal was sent to the PZT with the emission wavelength/frequency recorded using a wavemeter (High Finesse WS7), see Fig. 2(d). Both the thermal response of the cavity and the PZT tunability are currently limited by the thickness

Optics EXPRESS

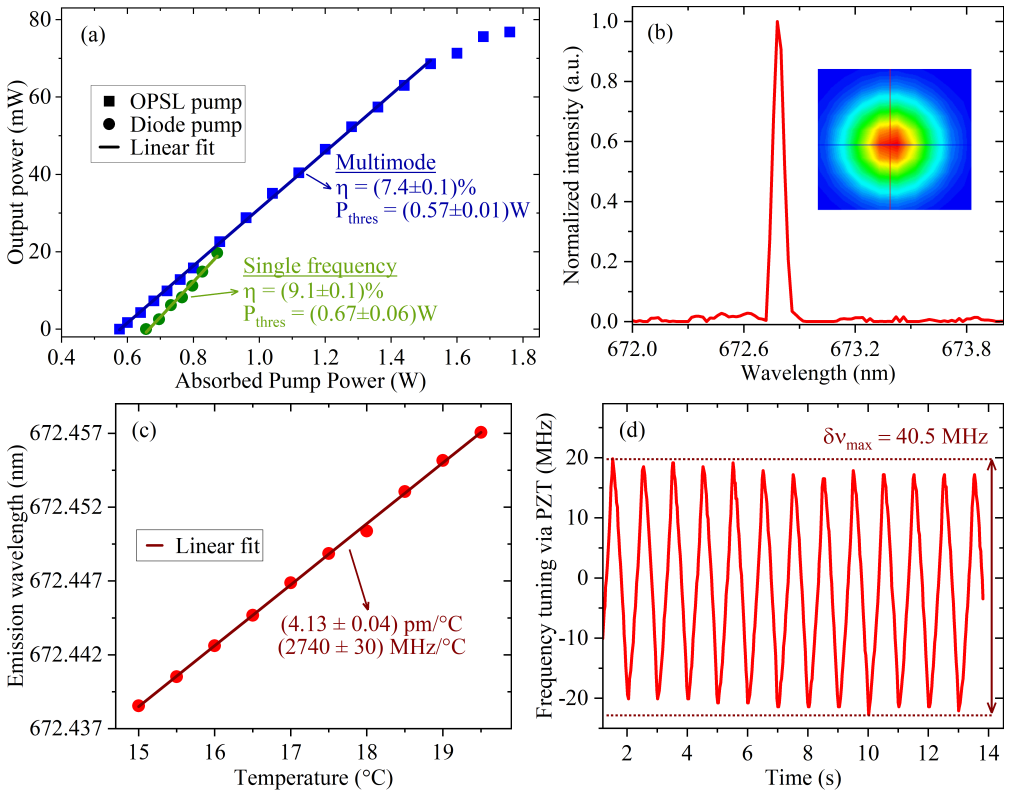

Fig. 2. (a) Monolithic VECSEL power transfer when pumped by a commercial OPSL (blue squares) and by a green diode laser (circles) in spot sizes of 65 and 50 µm, respectively. Commercial OPSL pump: a maximum multimode output power of 78 mW was measured with a threshold of (0.57 ± 0.01) W and conversion efficiency of (7.4 ± 0.1) %. Green diode-pump: single frequency operation with conversion efficiency of (9.1 ± 0.1) % and threshold of (0.67 ± 0.06) W. (b) Emission spectrum measured by an optical spectrum analyser (Anritsu MS9710C; resolution 0.05 nm). *Inset*: Monolithic VECSEL output beam profile. (c) Monolithic VECSEL wavelength tuning via brass mount temperature. A coarse tuning rate of 2740 MHz/°C was observed. (d) The shear PZT can be used to provide fast-response, finer wavelength tuning, up to 40.5 MHz.

of the off-the-shelf right-angle prism (25 mm). In this configuration, the oscillating field is situated 15 mm below the surface where the PZT is bonded, limiting the laser cavity frequency response, dynamic range and sensitivity [37]. Further miniaturization of the monolithic VECSEL cavity would allow for an increased frequency tuning range via the PZT, and would facilitate the implementation of active frequency stabilization techniques for further linewidth narrowing and frequency locking, as has been implemented with frequency stabilization in NPROs [38].

Finally, the polarization state of the monolithic VECSEL was measured with a polarization beam splitter (PBS) placed directly after the laser output, confirming that the laser oscillates in a stable s-polarized state. An extinction ratio of 100:1 was observed, which is limited by the PBS coatings.

Optics EXPRESS

4. Intensity and frequency noise analysis

The free-running relative intensity noise (RIN) of the monolithic VECSEL, with and without stabilization of the pump diode, is presented in Fig. 3. As a semiconductor laser, pump RIN is injected directly into the VECSEL intensity and frequency noise via the Henry factor, displaying a 1/f-noise behavior in the low frequencies [16], which can be seen in Fig. 3. When the pump intensity stabilization is switched on, a reduction of 30 dB in the noise floor is observed for frequencies below 1 kHz. A distinct peak is seen at 2.5 kHz which may have its origins in the delay period between detection of the VECSEL RIN and the delivery of the error signal to the CC. As noted in Section 3.1, the pump RIN detection could instead be reconfigured to use the Fresnel reflection for a faster response. Above 10 kHz a noise floor at around -128 dB can be observed with some additional high frequency noise peaks when compared to the RIN without diode stabilization, which is likely related to electronic noise introduced by the intensity stabilization electronics.

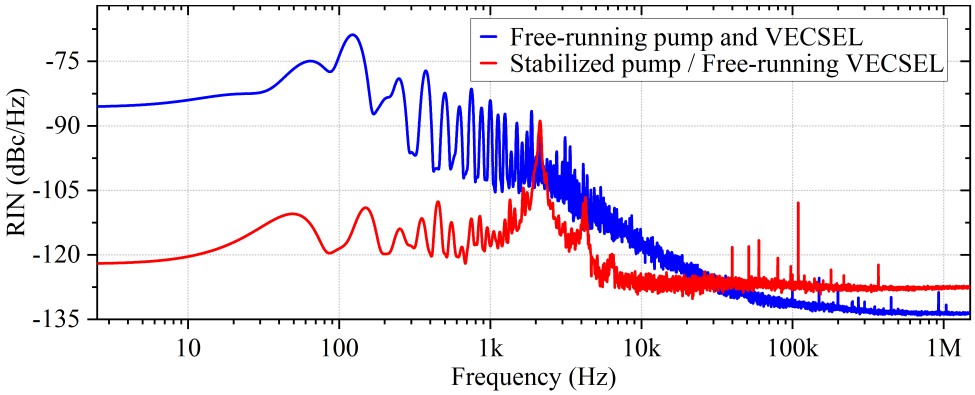

Fig. 3. Relative intensity noise for the diode-pumped monolithic VECSEL with (red) and without (blue) the pump intensity stabilization switched on. The free-running noise performance shows the typical 1/f behavior, which sees an approximate 30 dB reduction at low frequencies (< 1 kHz) when the stabilization is switched on. A dominant peak can be seen at 2.5 kHz which may be attributed to the temporal delay between the detection of the VECSEL RIN and the error signal delivered to the diode CC.

The diode-pumped monolithic VECSEL was coupled into a commercial scanning Fabry Perot (FP) cavity (FSR = 300 MHz, Finesse = 1 k) to confirm single frequency operation and to investigate the frequency noise performance of the laser. When tuned to match a resonance to the laser frequency, the transmission of the FP cavity was recorded over a sampling time of 1s, from which a one-sided frequency noise power spectral density (FNPSD) was calculated via auto-correlation and the Wiener-Khintchine theorem [39]. As expected, low frequency noise dominates the FNPSD presented in Fig. 4(a), with most being originated in the pump intensity noise injected in the VECSEL, and environmental noise. The main noise components for frequencies below 3 kHz are the AC electricity frequency (50 Hz) and its harmonics, and pump beam jitter from mechanical noise, translating to pump beam pointing errors, contributing to the peaks seen at 300 Hz and 1.7 kHz. The importance of pump intensity stabilization is highlighted in Fig. 4(a), which shows a strong reduction of ~32 dB in the VECSEL frequency noise across the observed frequency range, including a strong reduction in the peaks at low frequencies.

Also included in Fig. 4(a) is the β-separation line which is defined as $s_\beta(f) = 8f \ln 2/\pi^2$ [40] where f is the Fourier frequency. This line is used to divide the PSD into two regions: frequencies

Optics EXPRESS

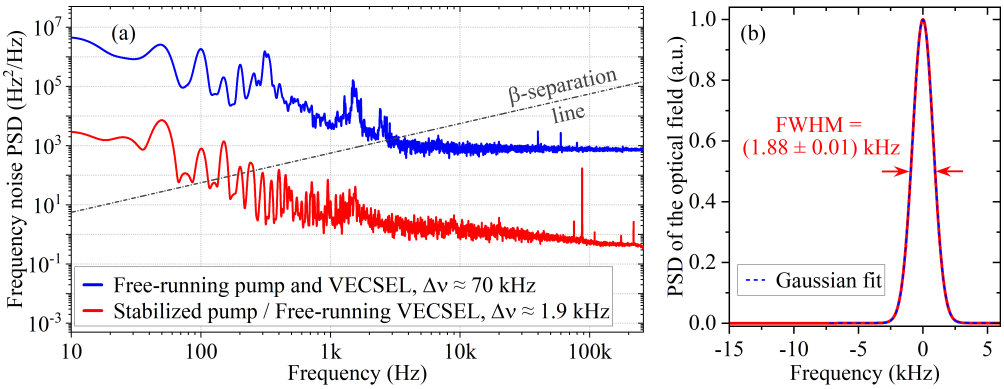

Fig. 4. (a) Frequency noise power spectral density traces for the free-running monolithic VECSEL when operating with the diode pump intensity stabilization switched on (red) and off (blue). The β separation line (black dot-dash) is also shown, separating the two regions that represent high frequency Lorentzian "wings" and the low frequency Gaussian line-shape. (b) Optical field reconstructed from autocorrelation and the Wiener-Khintchine theorem from the monolithic VECSEL PSD spectrum when the pump diode was intensity-stabilized.

above the separation line $s_\beta(f)<s_\nu(f)$ contribute to the central (Gaussian) part of the line shape and therefore the laser linewidth; frequencies below the β-separation line $s_\beta(f)>s_\nu(f)$ are considered too fast to affect the laser linewidth, only contributing to the wings (Lorentzian) of the line shape. Using the approximation $\delta\Delta\nu_{FWHM} \cong \sqrt{8(\ln 2)A}$ where A is the area under the PSD, the free-running linewidth for the monolithic VECSEL can be estimated to be 70 kHz, reducing to approximately 1.9 kHz when intensity stabilization of the diode pump is switched on. FNPSDs were also generated at shorter sampling times of around 1 ms with the linewidth estimated to be sub-kHz; however, for this range of sampling times the FNPSD data may be under-sampled at low Fourier frequencies, resulting in an insufficient number of points defining the area above the β-separation line to confidently report the linewidth [19]. Other techniques, such as beat note to an uncorrelated laser source emitting at the same wavelength with a similar or narrower linewidth, can be used in the future to fully characterize the monolithic VECSEL linewidth and noise. Nevertheless, the results presented here show a significant reduction in free-running linewidth when compared to previous results taken with a standard air-spaced cavity in the same lab environment, estimated at ~150 kHz [21], where pump intensity stabilization could not be implemented to the commercial OPSL as it is not possible to send feedback directly to the laser. This also compares favorably to NPROs, where active intensity stabilization is also employed to reduce the impact of the diode pump noise, resulting in free-running linewidths of (2-5) kHz [24,41].

5. Discussion

The prototype, diode-pumped, monolithic-cavity laser presented here offers a robust and compact platform for high brightness, kHz linewidth performance without frequency stabilization, for those applications that will benefit from high coherence lasers with reduced SWaP-C and reduced sensitivity to mechanical vibrations. There is also scope for further improvements in performance with more sophisticated engineering solutions, without significant changes to the fundamental cavity design. These will include optimization of the heat extraction from the VECSEL gain mirror, a reduction in thickness of the fused silica prism, the potential for using alternative optical crystals with a higher thermal conductivity, and improvements to each of the bonded interfaces. The result of which would reduce any interface-induced cavity loss and increase resilience against

Optics EXPRESS

thermal rollover for the monolithic VECSEL, resulting in higher output powers and stronger thermal stability. Power scaling could also be achieved with an adjusted resonator design to increase the laser mode size at the gain mirror and increase the thermal rollover point. While the available pump power from commercial green laser diodes is still an area of active development, we have previously demonstrated that red VECSELs can be pumped by high power blue diodes [35]; and for near- and mid-infrared VECSELs high power diode pumps are readily available [42].

With the robustness of a monolithic, class A cavity, the monolithic VECSEL offers orders-of-magnitude improvements in the free-running frequency noise and linewidth performance in comparison with other high-power semiconductor laser types. There are applications in quantum technology, such as the 689 nm strontium cooling transition, that require kHz linewidths that may be achievable in the future with a free-running, electronically-tunable monolithic VECSEL, rather than the additional complexity of stabilization to a separate frequency reference. This would dramatically reduce the SWaP-C of metrology systems that need linewidths of this order. For ultra-narrow (< Hz) laser linewidths additional stabilization will still be needed, and in the current embodiment active locking to a reference cavity or atomic reference could be implemented via the shear PZT. Furthermore, the miniaturization of the current embodiment, especially reducing the thickness of the prism, would allow for an increased tuning range and frequency response to external modulation, thus facilitating the implementation of more robust locking techniques.

An additional advantage to a monolithic cavity is the near perfect cavity alignment that is set by the tolerances of the optical components. Not only does this simplify optical alignment of the system, once the components are bonded together there are far fewer mechanical components to move when used in extreme environments, such as a space launch. This has contributed to the success of NPROs within this field as there are fewer points of failure in these laser systems. The same advantages will apply to a monolithic VECSEL with the additional advantage that, as the VECSEL is a planar absorber rather than a volume absorber, alignment and mode-matching of the pump beam can be arranged with higher tolerance. This could open up the possibility of extending the spectral coverage for space applications currently implementing NPROs, such as NASAs TES [28] and LISA [27] missions.

6. Conclusion

A novel monolithic VECSEL with an estimated free-running linewidth <1.9 kHz over 1s has been demonstrated. The monolithic cavity takes advantage of the intrinsically low noise VECSEL gain and total internal reflections inside a high precision right-angle prism to form an air-gap-free cavity for stable laser oscillation over long measurement times. The device was designed and constructed using commercially available optical components, offering a cost-effective solution to provide a robust monolithic platform for a high brightness, wavelength flexible laser technology. This monolithic design is applicable to the full range of III-V semiconductor gain materials with spectral coverage across the IR and visible spectrum. Future designs could employ more complex monolithic architectures, e.g. incorporating a nonlinear crystal for frequency conversion.

For integration with a neutral strontium atom clock, for example, the monolithic cavity can be combined with a VECSEL gain mirror to target either the 689 nm cooling transition or the 698 nm clock transition, such as those used in our previous work [21]. We have shown here that intensity-stabilized diode-pumping alone is sufficient to achieve free-running linewidth narrower than the strontium cooling transition (transition linewidth ~7 kHz), thus offering a much more compact solution to lasers that require external frequency stabilization [11,38]. For narrower linewidths, such as the clock transition, active feedback to the cavity via the PZT opens up the possibility of frequency locking techniques such as Pound-Drever-Hall [43].

Funding. Engineering and Physical Sciences Research Council (EP/L015315/1, EP/M013294/1, EP/T001046/1).

Optics EXPRESS

Disclosures. The authors declare no conflicts of interest.

Data availability. Data underlying the results presented in this paper are available in Ref. [44].

References

1. K. Yoshii, H. Sakagami, H. Yamamoto, S. Okubo, H. Inaba, and F.-L. Hong, "High-resolution spectroscopy and laser frequency stabilization using a narrow-linewidth planar-waveguide external cavity diode laser at 1063 nm," Opt. Lett. **45**(1), 129–132 (2020).
2. T. Mizuno, T. Kase, T. Shiina, M. Mita, N. Namiki, H. Senshu, R. Yamada, H. Noda, H. Kunimori, N. Hirata, F. Terui, and Y. Mimasu, "Development of the Laser Altimeter (LIDAR) for Hayabusa2," Space Sci. Rev. **208**(1-4), 33–47 (2017).
3. F. Sorrentino, K. Bongs, P. Bouyer, *et al.*, "A compact atom interferometer for future space missions," Microgravity Sci. Technol. **22**(4), 551–561 (2010).
4. R. Kaltenbaek, A. Acin, L. Bacsardi, *et al.*, "Quantum technologies in space," Exp. Astron. **51**(3), 1677–1694 (2021).
5. A. D. Ludlow, M. M. Boyd, J. Ye, E. Peik, and P. O. Schmidt, "Optical atomic clocks," Rev. Mod. Phys. **87**(2), 637–701 (2015).
6. M. G. Hansen, E. Magoulakis, Q.-F. Chen, I. Ernsting, and S. Schiller, "Quantum cascade laser-based mid-IR frequency metrology system with ultra-narrow linewidth and 1×10^{-13}-level frequency instability," Opt. Lett. **40**(10), 2289–2292 (2015).
7. B. J. Bloom, T. L. Nicholson, J. R. Williams, S. L. Campbell, M. Bishof, X. Zhang, W. Zhang, S. L. Bromley, and J. Ye, "An optical lattice clock with accuracy and stability at the 10^{-18} level," Nature **506**(7486), 71–75 (2014).
8. C. Grebing, A. Al-Masoudi, S. Dörscher, S. Häfner, V. Gerginov, S. Weyers, B. Lipphardt, F. Riehle, U. Sterr, and C. Lisdat, "Realization of a timescale with an accurate optical lattice clock," Optica **3**(6), 563–569 (2016).
9. S. Rothe, V. N. Fedosseev, T. Kron, B. A. Marsh, R. E. Rossel, and K. D. A. Wendt, "Narrow linewidth operation of the RILIS titanium: Sapphire laser at ISOLDE/CERN," Nucl. Instrum. Methods Phys. Res., Sect. B **317**, 561–564 (2013).
10. S. H. Xu, Z. M. Yang, T. Liu, W. N. Zhang, Z. M. Feng, Q. Y. Zhang, and Z. H. Jiang, "An efficient compact 300 mW narrow-linewidth single frequency fiber laser at 15 μm," Opt. Express **18**(2), 1249–1254 (2010).
11. M. G. Tarallo, N. Poli, M. Schioppo, D. Sutyrin, and G. M. Tino, "A high-stability semiconductor laser system for a ^{88}Sr-based optical lattice clock," Appl. Phys. B **103**(1), 17–25 (2011).
12. W. Jin, W. Jin, Q. F. Yang, L. Chang, B. Shen, H. Wang, M. A. Leal, L. Wu, M. Gao, A. Feshali, M. Paniccia, K. J. Vahala, and J. E. Bowers, "Hertz-linewidth semiconductor lasers using CMOS-ready ultra-high-Q microresonators," Nat. Photonics **15**(5), 346–353 (2021).
13. M. Corato-Zanarella, A. Gil-Molina, X. Ji, M. C. Shin, A. Mohanty, and M. Lipson, "Widely tunable and narrow-linewidth chip-scale lasers from near-ultraviolet to near-infrared wavelengths," Nat. Photon. **17**(2), 157–164 (2023).
14. M. Guina, A. Rantamäki, and A. Härkönen, "Optically pumped VECSELs: review of technology and progress," J. Phys. D: Appl. Phys. **50**(38), 383001 (2017).
15. F. Zhang, B. Heinen, M. Wichmann, C. Möller, B. Kunert, A. Rahimi-Iman, W. Stolz, and M. Koch, "A 23-watt single-frequency vertical-external-cavity surface-emitting laser," Opt. Express **22**(11), 12817–12822 (2014).
16. M. Myara, M. Sellahi, A. Laurain, A. Michon, I. Sagnes, and A. Garnache, "Noise properties of NIR and MIR VECSELs," in *Proc.SPIE 8606, Vertical External Cavity Surface Emitting Lasers (VECSELs) III*, 86060Q (2013).
17. A. L. Schawlow and C. H. Townes, "Infrared and optical masers," Phys. Rev. **112**(6), 1940–1949 (1958).
18. C. Henry, "Theory of the linewidth of semiconductor lasers," IEEE J. Quantum Electron. **18**(2), 259–264 (1982).
19. N. Von Bandel, M. Myara, M. Sellahi, T. Souici, R. Dardaillon, and P. Signoret, "Time-dependent laser linewidth: beat-note digital acquisition and numerical analysis," Opt. Express **24**(24), 27961–27978 (2016).
20. A. Laurain, C. Mart, J. Hader, J. V. Moloney, B. Kunert, and W. Stolz, "15 W single frequency optically pumped semiconductor laser with sub-megahertz linewidth," IEEE Photon. Technol. Lett. **26**(2), 131–133 (2014).
21. P. H. Moriya, Y. Singh, K. Bongs, and J. E. Hastie, "Sub-kHz-linewidth VECSELs for cold atom experiments," Opt. Express **28**(11), 15943–15953 (2020).
22. T. J. Kane and R. L. Byer, "Monolithic, unidirectional single-mode Nd:YAG ring laser," Opt. Lett. **10**(2), 65–67 (1985).
23. G. Lin and Y. K. Chembo, "Monolithic total internal reflection resonators for applications in photonics," Optical Materials: X **2**, 100017 (2019).
24. E. Hernan, Q. Yueming, P. Ilya, M. Patrick, and W. James, "Reliable optical pump architecture for highly coherent lasers used in space metrology applications," in *Proc.SPIE 7734, Optical and Infrared Interferometry II*, 77342B (2010).
25. A. C. Nilsson, E. K. Gustafson, and R. L. Byer, "Eigenpolarization theory of monolithic nonplanar ring oscillators," IEEE J. Quantum Electron. **25**(4), 767–790 (1989).
26. J. E. Hastie, J.-M. Hopkins, C. W. Jeon, S. Calvez, D. Burns, M. D. Dawson, R. Abram, E. Riis, A. I. Ferguson, W. J. Alford, T. D. Raymond, and A. A. Allerman, "Microchip vertical external cavity surface emitting lasers," Electron. Lett. **39**(18), 1324–1326 (2003).

Optics EXPRESS

27. N. Kenji, W.Y. Anthony, J. Hua, A.M. Scott, M. Frankie, E.F. Molly, B.C. Jordan, and A.K. Michael, "Laser system development for the LISA (Laser Interferometer Space Antenna) mission," in *Proc.SPIE 10896, Solid State Lasers XXVIII: Technology and Devices*, 108961 H (2019).
28. C.G. Asbury, L.I. Dorsky, N.M. Nerheim, S. Forouhar, D.M. Rider, E.Y. Chu, B.M. Fisher, R.S. Valencia, M.R. Montero, and T.J. Kane, "Space- and ground-based non-accelerated long lifetime data for ruggedized commercial NPRO lasers," in *Proc.SPIE 11180, International Conference on Space Optics*, 1118019 (2019).
29. T. D. Shoji, W. Xie, K. L. Silverman, A. Feldman, T. Harvey, R. P. Mirin, and T. R. Schibli, "Ultra-low-noise monolithic mode-locked solid-state laser," Optica **3**(9), 995–998 (2016).
30. S. Calvez, J. E. Hastie, M. Guina, O. G. Okhotnikov, and M. D. Dawson, "Semiconductor disk lasers for the generation of visible and ultraviolet radiation," Laser Photonics Rev. **3**(5), 407–434 (2009).
31. A. J. Kemp, G. J. Valentine, J. Hopkins, J. E. Hastie, S. A. Smith, S. Calvez, M. D. Dawson, and D. Burns, "Thermal management in vertical-external-cavity surface-emitting lasers: finite-element analysis of a heatspreader approach," IEEE J. Quantum Electron. **41**(2), 148–155 (2005).
32. A. J. Kemp, G. J. Friel, T. K. Lake, R. S. Conroy, and B. D. Sinclair, "Polarization effects, birefringent filtering, and single-frequency operation in lasers containing a birefringent gain crystal," IEEE J. Quantum Electron. **36**(2), 228–235 (2000).
33. I. Friel, S. L. Clewes, H. K. Dhillon, N. Perkins, D. J. Twitchen, and G. A. Scarsbrook, "Control of surface and bulk crystalline quality in single crystal diamond grown by chemical vapour deposition," Diamond Relat. Mater. **18**(5-8), 808–815 (2009).
34. T. Fördös, H. Jaffrès, K. Postava, M. S. Seghilani, A. Garnache, J. Pištora, and H. J. Drouhin, "Eigenmodes of spin vertical-cavity surface-emitting lasers with local linear birefringence and gain dichroism," Phys. Rev. A **96**(4), 043828 (2017).
35. P. H. Moriya, R. Casula, G. A. Chappell, D. C. Parrotta, S. Ranta, H. Kahle, M. Guina, and J. E. Hastie, "InGaN-diode-pumped AlGaInP VECSEL with sub-kHz linewidth at 689 nm," Opt. Express **29**(3), 3258–3268 (2021).
36. A. Laurain, J. Hader, and J. V. Moloney, "Modeling and optimization of transverse modes in vertical-external-cavity surface-emitting lasers," J. Opt. Soc. Am. B **36**(4), 847–854 (2019).
37. W. Holzapfel, S. Neuschaefer-Rube, and M. Kobusch, "High-resolution, very broadband force measurements by solid-state laser transducers," Measurement **28**(4), 277–291 (2000).
38. P. Kwee, C. Bogan, K. Danzmann, M. Frede, H. Kim, P. King, J. Pöld, O. Puncken, R. L. Savage, F. Seifert, P. Wessels, L. Winkelmann, and B. Willke, "Stabilized high-power laser system for the gravitational wave detector advanced LIGO," Opt. Express **20**(10), 10617–10634 (2012).
39. M. Tröbs and G. Heinzel, "Improved spectrum estimation from digitized time series on a logarithmic frequency axis," Measurement **39**(2), 120–129 (2006).
40. G. Di Domenico, S. Schilt, and P. Thomann, "Simple approach to the relation between laser frequency noise and laser line shape," Appl. Opt. **49**(25), 4801 (2010).
41. Z. Bai, Z. Zhao, M. Tian, D. Jin, Y. Pang, S. Li, X. Yan, Y. Wang, and Z. Lu, "A comprehensive review on the development and applications of narrow-linewidth lasers," Microw. Opt. Technol. Lett. **64**(12), 2244–2255 (2022).
42. H. Liu, G. Gredat, G. Baili, F. Gutty, F. Goldfarb, I. Sagnes, and F. Bretenaker, "Noise investigation of a dual-frequency VECSEL for application to cesium clocks," J. Lightwave Technol. **36**(18), 3882–3891 (2018).
43. R. W. P. Drever, J. L. Hall, F. V. Kowalski, J. Hough, G. M. Ford, A. J. Munley, and H. Ward, "Laser Phase and Frequency Stabilization Using an Optical-Resonator," Appl. Phys. B **31**(2), 97–105 (1983).
44. M. Lee, P.H. Moriya, and J.E. Hastie, "Data for: Monolithic VECSEL for stable kHz linewidth," University of Strathclyde (2023) http://doi.org/10.15129/a322a11e-1729-4339-9279-965f69330a44.